HHS Public Access

Author manuscript

Cell Rep. Author manuscript; available in PMC 2018 April 11.

Published in final edited form as:

Cell Rep. 2018 March 20; 22(12): 3351–3361. doi:10.1016/j.celrep.2018.02.081.

Silk Fibroin Films Facilitate Single-Step Targeted Expression of Optogenetic Proteins

Skyler L. Jackman[1,3,4], **Christopher H. Chen**[1,3], **Selmaan N. Chettih**[1], **Shay Q. Neufeld**[2], **Iain R. Drew**[1], **Chimuanya K. Agba**[1], **Isabella Flaquer**[1], **Alexis N. Stefano**[1], **Thomas J. Kennedy**[1], **Justine E. Belinsky**[1], **Keiramarie Roberston**[2], **Celia C. Beron**[1], **Bernardo L. Sabatini**[2], **Christopher D. Harvey**[1], and **Wade G. Regehr**[1,5,*]

[1]Department of Neurobiology, Harvard Medical School, Boston, MA 02115, USA

[2]Department of Neurobiology, Howard Hughes Medical Institute, Harvard Medical School, Boston, MA 02115, USA

SUMMARY

Optical methods of interrogating neural circuits have emerged as powerful tools for understanding how the brain drives behaviors. Optogenetic proteins are widely used to control neuronal activity, while genetically encoded fluorescent reporters are used to monitor activity. These proteins are often expressed by injecting viruses, which frequently leads to inconsistent experiments due to misalignment of expression and optical components. Here, we describe how silk fibroin films simplify optogenetic experiments by providing targeted delivery of viruses. Films composed of silk fibroin and virus are applied to the surface of implantable optical components. After surgery, silk releases the virus to transduce nearby cells and provide localized expression around optical fibers and endoscopes. Silk films can also be used to express genetically encoded sensors in large cortical regions by using cranial windows coated with a silk/virus mixture. The ease of use and improved performance provided by silk make this a promising approach for optogenetic studies.

In Brief

Jackman et al. show that coating optical implants with silk fibroin mixed with AAV allows single-step implantation and expression of optogenetic proteins like channelrhodopsin and GCaMP.

*Correspondence: wade_regher@hms.harvard.edu.

[3]These authors contributed equally

[4]Present address: Vollum Institute, Oregon Health and Science University, Portland, OR 97239, USA

[5]Lead Contact

SUPPLEMENTAL INFORMATION

Supplemental Information includes two figures and three movies and can be found with this article online at https://doi.org/10.1016/j.celrep.2018.02.081.

AUTHOR CONTRIBUTIONS

S.L.J. and W.G.R. conceived experiments. S.L.J., C.H.C., I.R.D., C.K.A., I.F., A.N.S., T.J.K., and J.E.B. made implants, performed surgeries, and analyzed expression. K.R. implanted GRIN lenses and collected microendoscope videos that were analyzed by S.Q.N. and C.C.B. *In vivo* 2-photon imaging was acquired and analyzed by C.H.C., I.F., and S.N.C. Microendoscope experiments were supervised by B.L.S. In vivo 2-photon imaging experiments were supervised by C.D.H. Behavioral assays were performed by S.L.J. and C.H.C. S.L.J., C.H.C., and W.G.R. wrote the manuscript.

DECLARATION OF INTERESTS

The authors declare no competing interests.

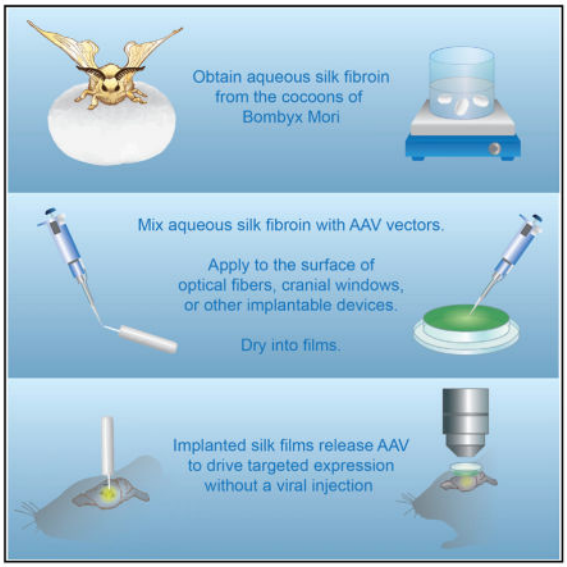

INTRODUCTION

Optogenetic approaches to monitor and manipulate neural activity provide crucial insights into how neural circuits drive behavior (Fenno et al., 2011; Knöpfel, 2012). Optogenetic proteins can be expressed using transgenic animals (Zeng and Madisen, 2012) or electroporation, but adeno-associated virus (AAV) remains the most flexible, economical, and widely used means of targeting spatially and genetically defined populations of neurons (Packer et al., 2013). Stereotaxic AAV injections are highly effective at expressing proteins in target brain regions. However, following AAV injection, a second surgical step is required when an optical fiber is used for light delivery or when an endoscope is used to monitor fluorescence (Resendez et al., 2016; Sparta et al., 2011). The requirement for two surgical steps reduces the success rate of experiments by increasing the likelihood of tissue damage and by increasing the probability that either the virus or the optical device is incorrectly targeted. Specialized optical implants with microfluidic channels have been used to overcome this problem by allowing the delivery of both light and AAV vectors to the brain in a single surgery (Jeong et al., 2015; Park et al., 2017). However, this approach has not been widely applied, because it requires specialized devices that are not commercially available. AAVs are also used to express proteins for imaging through implanted cranial windows. To achieve expression across the large area beneath imaging windows, multiple injections are required and the resulting expression is usually uneven, which is a significant drawback for such studies.

Here, we deliver optogenetic viral vectors using films of silk fibroin, derived from the cocoon of *Bombyx mori* (Vepari and Kaplan, 2007), to eliminate the need for stereotaxic injections. Fibroin is a biocompatible material that has been shown to induce minimal immunogenic responses in tissues, including the CNS (Fernández-García et al., 2016; Kim et al., 2010; Rock-wood et al., 2011; Tang et al., 2009; Vepari and Kaplan, 2007). Materials made from fibroin can be tailored in their degree of solubility and engineered into forms

ranging from low-density hydrogels to durable ceramics (Rockwood et al., 2011). Importantly, fibroin-based materials can encapsulate and preserve biomolecules such as vaccines and viral vectors (Pritchard et al., 2012; Zhang et al., 2012), and they can be used to release those reagents into tissue after implantation (Wilz et al., 2008; Zhang et al., 2011).

We present a straightforward procedure for coating optical devices with films composed of silk fibroin and AAV vectors that eliminates the need for separate injections. By depositing a mixture of silk and AAV-ChR2 onto the tip of standard optical fibers (Sparta et al., 2011), fiber implantation leads to expression near the fiber tip. Coating tapered optical fibers (Pisanello et al., 2017) with a silk and AAV film produces uniform expression along the fiber that takes full advantage of the ability to illuminate at different depths with these specialized fibers. We show that with a single, simple surgery, it is possible to reliably elicit behavioral responses with both tapered and conventional fibers. For functional imaging, we demonstrate that silk and AAV-GCaMP deposited on the tip of endoscopes (Resendez et al., 2016) allows transduction of cells for calcium imaging *in vivo* without the need for additional stereotaxic injections. Similarly, coating cranial windows (Goldey et al., 2014; Holtmaat et al., 2009) with silk and AAV results in broad expression across the surface of the brain that greatly facilitates 2-photon *in vivo* GCaMP imaging. In summary, silk/AAV films greatly simplify the implementation of optogenetic experiments, lead to improved experimental throughput, and promise to be an important technical advance in the application of optogenetic approaches.

RESULTS

Silk Films Deliver AAVs around Implanted Optical Fibers

For many optogenetic applications, a viral vector that expresses a light-activated opsin is injected into a target region, and then an optical fiber is implanted into that region for activation or inhibition of transduced neurons (Figure 1A). This approach has several limitations. First, this procedure involves physically perturbing the brain twice. Second, the injection and the optical fiber must both hit the target region, reducing the likelihood of success and increasing experimental cost and time (Figure 1A1). Alignment issues are often partially overcome by increasing viral titer and injection volume to obtain expression in larger areas (Figure 1A2), but this approach can result in optogenetic activation of unwanted brain regions. We therefore wanted to develop a means of overcoming these difficulties, and using silk as a scaffold to hold virus to the fiber tip seemed like a possible solution.

We began by preparing aqueous silk fibroin as previously described (Rockwood et al., 2011). This silk fibroin solution (5%–7.5% w/v, which we will refer to as silk) was mixed 1:1 with stock-titer AAV-GFP vector (Experimental Procedures). This mixture was then applied directly to a fiber tip, dried, and vacuum desiccated overnight at 4°C (Figure 1B). We experimented with several ways to apply the silk/AAV mixture to the tip of the optical fiber. Applying large volumes from the top often resulted in droplets sliding down the shaft of the optic fiber (Figure 1C). Applying large volumes of silk directly from the bottom was more successful, though it resulted in a larger silk pellet when the droplet was dried (Figure 1D). The most successful approach was to repeatedly apply 10-nL droplets of silk/AAV

from the bottom of the optical fiber, waiting 1 min for the mixture to dry, and repeating this procedure until the desired total volume was achieved (Figure 1E).

We tested the ability of this approach to achieve focal labeling by implanting optical fibers tipped with a silk/AAV-GFP mixture into the striatum. These produced GFP expression that was confined to the tip of the optical fiber (Figures 1F and 1H). To determine whether silk was necessary for focal expression, we performed similar experiments with optical fibers that only had AAV-GFP deposited at the tip (Figures 1G and 1H). AAV-only films resulted in expression both at the tip of the fiber and all along the path of the optical fiber as it progressed through the cortex to the striatum (Figures 1G and 1H). This suggests that the inclusion of silk produces films that do not release significant amounts of virus during the act of implantation but rather release virus slowly near the tip of the fiber after surgery. We were able to systematically vary the amount of expression near the tip of the optical fiber by titrating the amount of the silk/AAV mixture applied to the tip (Figures 1I, 1J, and S1). We found that the method of silk application shown in Figure 1E was important to confine expression to a region near the tip, which presumably reflected silk films adhering reliably to the tip of the optical fiber. When silk was applied from the top (Figure 1C), or in a single application from the bottom (Figure 1D), expression at the tip was variable and was often not confined to the tip, suggesting that the silk/AAV film did not remain adhered to the tip.

For this study, we performed all the surgeries within 48 hr of manufacturing the silk/AAV-coated implants. However, to test the possibility that silk/AAV-coated devices might be manufactured in advance and remain effective, we implanted a small subset of fibers 1 week after coatings were applied. These fibers were stored in a vacuum chamber at 4°C. We saw a small but statistically insignificant difference in the extent of expression compared to similar, freshly manufactured implants (<48 hr: 0.59 ± 0.05 mm^2 [n = 7] striatal expression area versus 1 week: 0.43 ± 0.05 mm^2 [n = 5], p = 0.07, Wilcoxon rank sum). These results indicate that it is possible to prepare optical fibers coated with silk/AAV mixtures well in advance for subsequent use.

Silk/AAV-Coated Optical Fibers Can Be Used to Reliably Trigger Specific Behaviors

We tested the ability of silk/AAV-coated optical fibers to control behavior by assessing our ability to evoke escape responses by stimulating the anterior hypothalamic nucleus (AHN). Both electrical and optogenetic stimulation of this area can elicit a robust escape jumping behavior in rodents (Lammers et al., 1988; Wang et al., 2015). However, in a previous study that expressed ChR2 in the AHN by stereotaxic injection, optogenetic stimulation induced escape jumping in only 5 of 8 animals, and among those animals that responded, light elicited escape jumps in less than 60% of trials (Wang et al., 2015). We targeted silk/AAV-ChR2-YFP-coated implants to the AHN, an area at the most ventral edge of the brain (Figure 2A). Accordingly, we used 100 nL of silk/AAV to maximize transduction and make implant location the sole determinant of eliciting consistent behaviors. 2–3 weeks after implantation, we used optical stimulation similar to what was used previously (Wang et al., 2015) (20 Hz, 1 ms for 60 s) and elicited reliable and repeatable escape jumping in all 11 animals that received silk/AAV-coated optical fibers (Figure 2B; Movie S1). On average, light evoked more than 10 jumps per minute and always evoked multiple jumps (Figure 2C).

For most mice, where optical fibers were located within 0.3 mm of the AHN, low light intensities were sufficient to elicit jumps (Figure 2D). For 3 mice with implants >0.5 mm away from the center of the AHN, higher light intensities were required (Figure 2D). These results illustrate the ease of use and consistent performance of silk/AAV-coated optical fibers for optogenetic studies.

Silk/AAV-Coated Tapered Fibers Reliably Drive Expression across the Fiber Axis

Tapered optical fibers (Figure 3A, left) were recently developed to provide a less invasive means of light activation *in vivo*, allow illumination of large brain regions, and enable selective illumination of different depths with the same fiber (Pisanello et al., 2017). It is desirable to have uniform expression of an opsin along the entire length of the taper, but this is difficult to achieve reliably with injections. We therefore tried to obtain labeling by coating optical fibers with silk/AAV-GFP (Figure 3A, middle). When implanted into the striatum, these coated optical fibers achieved robust GFP expression along the fiber's length (Figure 3A, right). The use of silk/AAV also permits expression of distinct opsins at different depths along the fiber. We coated a tapered fiber with silk/AAV-GFP near the tip and silk/AAV-RFP along the shaft and obtained spatially segregated fluorescence within the striatum (Figure 3B). This result exemplifies the precise spatial targeting that can be achieved with silk and illustrates an approach that could be particularly powerful when combined with the ability of tapered fibers to selectively illuminate different depths along the fiber, potentially with different wavelengths of light.

To test the functional utility of these tapered fibers, we coated fibers with silk/AAV9-Syn-ChR2-YFP and implanted them in the motor cortex (Figure 3C). Optogenetic stimulation of the motor cortex has been previously demonstrated to elicit increased locomotion and turning in the direction contralateral to the implant (Gradinaru et al., 2007; Montgomery et al., 2015). Consistently, optogenetic stimulation using tapered fibers implanted in the right motor cortex (20 Hz, 5 ms, ~3 mW, 473 nm for 5 s) increased locomotion velocity and induced leftward turning (n = 3 mice) (Figures 3D–3F; Movie S2). Together, these experiments suggest that labeling achieved by coating tapered fibers with silk/AAV provides a simple means of reliably evoking behavioral responses

Ca^{2+} Imaging in Freely Behaving Animals with Silk/AAV-Coated GRIN Lenses

The recent development of miniaturized head-mounted micro-endoscopes greatly expands the ability to optically monitor neuronal activity deep in the brains of freely moving animals (Flusberg et al., 2008; Resendez et al., 2016). Here, a gradient refractive index (GRIN) lens is implanted above the brain region of interest and connected to a lightweight head-mounted camera with its own light source. The microendoscope can then image a fluorescent reporter of neuronal activity such as the genetically encoded calcium indicator GCaMP. As with other *in vivo* optogenetic applications, genetically encoded calcium indicators are often expressed by injecting AAV vectors prior to GRIN lens implantation. However, it can be difficult to align the GRIN lens to the injection site, and because of the large diameter of many GRIN lenses (up to 1 mm), it can also be difficult to obtain expression across the entire field of view. Moreover, the additional surgery for AAV injection increases the risk of tissue damage in the region of interest.

We therefore evaluated whether silk/AAV-GCaMP could be used to coat the surface of a GRIN lens to label neurons uniformly over the entire imaging region and eliminate the need for injections. We coated microendoscope lenses with a suspension of silk and AAV-GCaMP6s. A 1-μL droplet of silk/AAV suspension was applied to the surface GRIN lenses. After several hours of drying at room temperature, a ~100-μm-thick film remained on the lens surface. Lenses were implanted film-side down into the dorsal striatum (Figure 4A). GCaMP expression was evident 7 days after surgery, and after 2 weeks, there was sufficient GCaMP expression to resolve fluorescence transients across a large area of the field of view. Images obtained with GRIN lenses are not high resolution, and the image quality obtained when silk/AAV was used to label cells were qualitatively similar to those obtained when conventional injections of AAV were used to label cells. This indicates that for this application the presence of silk does not noticeably degrade image quality. Due to the poor axial resolution of 1-photon microendoscopes, it is difficult to distinguish individual GCaMP-expressing cells without the use of a time-series-based segmentation algorithm (Figure 4A, inset). After applying such an algorithm (Zhou et al., 2016) (Figure 4B), we could resolve calcium transients in a large number of neurons during animal locomotion (Figure 4C). These experiments establish that the silk/AAV approach is well suited to labeling cells for functional imaging with GRIN lenses while eliminating the need for injections of AAV.

Widespread Expression Using Silk/AAV-Coated Cranial Windows

While microendoscopes are useful for imaging neuronal activity in freely moving animals and deep brain regions, 2-photon imaging through cranial windows offer multiple advantages for *in vivo* imaging of superficial brain structures. Chronically implanted cranial windows provide far larger fields of view. Windows range from 3-mm circles (Goldey et al., 2014; Holtmaat et al., 2009) to large “crystal skulls” designed to replace the entire dorsal cranium and permit optical monitoring of millions of neurons (Kim et al., 2016).

Due to the large tissue volumes that can be imaged beneath cranial windows, as many as 18 viral injections (Runyan et al., 2017) are used to obtain expression of fluorescent indicators across the imaging field (Figure 5A). This approach often results in uneven expression patterns, and each injection site can cause tissue damage. Moreover, the sheer number of stereotaxic injections is time-consuming and laborious and decreases experimental throughput. In principle, silk/AAV-coated windows could deliver virus evenly across the imaging field to produce more uniform expression, cause less tissue damage, and drastically reduce the time required for surgeries (Figure 5B). However, the dura and pia constitute physical barriers between skull windows and cortical neurons. Viral particles released from the surface of a skull window might be unable to penetrate to the underlying tissue and transduce neurons.

To test whether silk/AAV-coated windows can deliver virus over broad cortical areas, a silk/AAV suspension was pipetted onto 3-mm-diameter cranial windows (Goldey et al., 2014; Holtmaat et al., 2009) and allowed to dry for several hours at room temperature prior to implantation. To distinguish individual transduced cells *in vivo*, we used an AAV vector that expresses a nuclear-tagged GFP (AAV-HI-EGFP). The dura was removed beneath the

window to ensure that viral particles could reach the cortical surface. 2–3 weeks after implantation, in vivo 2-photon imaging revealed strong labeling of cell bodies in layer 2/3 of the cortex (Figure 5C, left). GFP expression was remarkably uniform across the entire area of the cranial window. Unexpectedly, GFP expression extended across almost the entire cortical hemisphere (Figure 5C, middle). Cortical slices cut from these brains confirmed the large extent of labeling and revealed that many neurons were labeled deep in the cortex. Because our aim with windows was simply to drive expression over a broad area and not to restrict the release of virus to a certain area as with fiber implants, we wondered whether silk was necessary for this application. We therefore performed experiments with cranial windows coated with AAV alone. Several weeks after implantation, *in vivo* 2-photon imaging revealed far less expression than for silk/AAV experiments (Figure 5D), suggesting that silk is an important requirement for substantial expression.

We next assessed whether silk/AAV-coated cranial windows can be used to express GCaMP for functional imaging of neuronal activity *in vivo*. We implanted cranial windows coated with silk/AAV-GCaMP over the primary motor cortex (Figure 6A) and performed a durectomy beneath the window. Durectomies can improve the quality of 2-photon images and are sometimes used for *in vivo* GCaMP imaging (Goldey et al., 2014; Smith and Fitzpatrick, 2016). However, durectomies are sometimes avoided because they increase the risk of damaging the superficial cortex (Mostany and Portera-Cailliau, 2008). To test whether durectomies are required for virus coated onto windows to transduce the brain, we implanted silk/AAV-coated windows without performing durectomies in a subset of animals (Figures 6B, 6C, and S2). Remarkably, silk/AAV-coated windows drove some GCaMP expression even when the dura was not removed during the cranial window surgery. The labeling was not as robust as when the dura was removed but maintains the possibility that one might refine approaches to obviate the need for a durectomy. This might prove useful for approaches where minimally invasive expression of vectors through the dura is necessary. Finally, we again tested whether silk was required by coating some windows with a suspension of virus alone but performing durectomies. We assessed expression by waiting more than 3 weeks and cutting cortical slices (Figure 6B). Extensive expression that extended at least 800 μm below the surface of the cortex was seen in all animals in which silk/AAV was used in combination with a durectomy (Figure 6B, top, Figure 6C). Very little fluorescence was apparent when only AAV was used in combination with a durectomy, reinforcing the importance of silk.

Imaging experiments were performed on animals in which silk/AAV was used in combination with a durectomy. Several weeks after implantation, we performed *in vivo* 2-photon imaging on anesthetized, head-fixed mice. Low-power, 2-photon images of the entire cranial window revealed extensive GCaMP labeling (Figure 6D, left). At higher magnification, individual cell bodies were apparent (Figure 6D, middle), and calcium transients could be recorded from a large number of cells (Figure 6D, right; Movie S3).

DISCUSSION

We have shown that silk is a beneficial tool for many different types of optogenetic studies. Its primary virtue is that it eliminates the need for a second step to inject AAVs into the

brain. Furthermore, the silk approach leads to consistent expression that is spatially aligned with the implanted optical device and also enables titratable expression for both small and large brain regions. The simplicity of the approach suggests that it will become a powerful aid to future optogenetic studies.

Advantages of Silk in Specific Optogenetic Applications

Using silk with conventional optical fibers offers several important advantages. First, expression can be perfectly aligned with the fiber and restricted to the tip without the need for a separate surgery, making these types of experiments easier to perform and more reliable. This was illustrated by our ability to evoke robust behaviors using optogenetic activation, even when targeting a small hypothalamic nucleus located in a very ventral region of the brain. Another promising feature is the ability to control the number of cells transduced near the tip of the fiber, allowing a reasonable estimate of how many neurons are activated and their precise location. This is not generally possible with transgenic animals or with typical AAV experiments, where more extensive expression makes it difficult to determine which cells are influenced by light and the influence of light as a function of distance. Moreover, compared to other methods for implanting optical devices and delivering viral vectors in a single step, silk films require less specialized components and are far easier to implement (Jeong et al., 2015; Park et al., 2017). Silk films can be applied to the tip of optical fibers and microscope lenses by the same injection methods used for stereotaxic injections. Fibroin acts as an adhesive (Tao et al., 2012) and thus films bind stably even to small optical fibers. Multiple optical implants can be manufactured and coated at the same time, at least a day in advance of surgeries. Importantly, the barrier to using silk films has recently become even lower. During the course of this study we needed to produce our own aqueous fibroin stocks approximately once every 3 months. However, 5% w/v aqueous silk fibroin has recently become commercially available and appears to perform similarly to our own fibroin stocks.

Silk makes it straightforward to take full advantage of the technical benefits of tapered fibers: their minimally invasive nature and their ability to illuminate specific depths along the fiber. Silk/AAV can be used to label around the entire fiber, and this permits optical control of activity at different depths. Such labeling normally requires a series of invasive injections that are difficult to align to the tapered fiber. Experiments in which we implanted fibers in the motor cortex to increase speed and promote turning illustrate how simple it is to use silk-coated fibers to control behavior. Our ability to simply and precisely control the expression of different opsins as a function of depth also enables new types of studies that can be performed with tapered fibers.

We demonstrate that silk can be used to facilitate monitoring neuronal activity. Appropriate labeling with the desired activity indicator can be achieved simply by coating the surface of an endoscope with silk/AAV. Although we have emphasized the use of conventional and tapered fibers for optical control of neuronal activity, they could also be used for fiber-based photometric measurements.

We further demonstrate the ability to label large regions of cortex by coating the underside of a cranial window with silk/AAV. The standard approach is to remove the dura below the

optical window to improve imaging resolution. When silk/AAV was applied to a cortex following a durectomy, we observe robust expression across the cortex. This has the potential to simplify experiments and avoid invasive time-consuming procedures such as multiple injections within the imaging field, and it promises to provide more uniform expression than can be typically achieved. Although other methods for driving widespread expression have recently been developed using new transgenic lines (Madisen et al., 2015) and AAV serotypes (Deverman et al., 2016), conventional AAV vectors remain the more flexible approach for driving neuronal expression, and silk films can help evenly distribute these vectors to drive widespread expression only in the brain region of interest.

Future Methodological Refinement

These initial steps in using silk to aid in optogenetic studies are promising, and it is likely that future studies will refine these approaches and extend the range of applications. Silk-fibroin-based materials can be prepared in many ways, and it is possible that superior performance is possible with alternative preparation methods. Fibroin can also be used to make hydrogels, nanofibers, microsopheres, and even sponges (Rockwood et al., 2011; Vepari and Kaplan, 2007), and these different preparations may lead to superior performance for specific applications. One of the potential benefits of using silk to deliver AAVs on optical fibers, endoscopes, and windows is that silk has been reported to stabilize and protect viruses and other biomolecules. Our initial tests found that fibers could be implanted a week after preparation and still effectively transduce neurons. This suggests that it might be possible to store coated implants for long periods of time without significant loss of viral efficacy. Also, numerous studies have highlighted the different properties of silk films prepared under various conditions, and it remains to be seen whether viral release could be improved by treating films to change their microscopic structure (Rockwood et al., 2011). Future studies will be needed to determine the best conditions to stabilize AAVs with silk and allow prolonged storage of prepared films.

In testing silk with cranial windows, we serendipitously discovered that silk somehow facilitates transduction of cortical neurons without removing the dura. We obtained sufficient GCaMP expression to allow us to record activity in layer 2/3 neurons, although the expression was far inferior to that observed when the dura was removed. Further studies are required to understand how such labeling is achieved and determine whether it is possible to improve GCaMP expression for such experiments. Recently, surfaces coated with silk microneedles were shown to release vaccine after being applied to the skin (Stinson et al., 2017). This technique could potentially be applied to cranial windows to more effectively deliver AAV across the dura without causing damage to the underlying cortical tissue.

Finally, for this study, we chose silk fibroin because it is cheap and easily purified and because it has been shown to produce minimal immunogenic responses in tissue (Fernández-García et al., 2016; Kim et al., 2010; Rockwood et al., 2011; Tang et al., 2009; Vepari and Kaplan, 2007). It has the added advantage that it is now commercially available. Numerous other polymeric materials have also proven capable of forming scaffolds that encapsulate viruses and other biomolecules and release them in a stimulus-specific manner (Jang et al., 2011; Zeng et al., 2012). These include self-assembling peptides, proteins like collagen and

fibrin, and small-molecule synthetic polymers such as polyethylene glycol and poly(lactic-co-glycolic acid) (PLG) scaffolds (Jang et al., 2011; Schek et al., 2004). To date, there have been no side-by-side comparison of the relative efficacy of these materials for controlled release of viral vectors into tissue. More research is needed to determine whether any of these molecules offer advantages over silk fibroin.

Future Applications of Silk/AAV Materials

It is likely that these approaches can be extended to other types of viral expression vectors, including lentivirus and helper-dependent adenoviral vectors that allow the delivery of larger payloads and next-generation, rapidly expressing, transsynaptic herpes simplex (Lo and Anderson, 2011) and rabies viruses (Reardon et al., 2016). Although we have focused on optically activated proteins and calcium sensors, sensors for voltage and second messengers other than calcium can also be expressed. It could also be useful to use silk/AAV to express or knockdown proteins (via small hairpin RNA [shRNA] or clustered regularly interspaced short palindromic repeats [CRISPR]) specifically around implant sites. Chemogenetic tools like designer receptors exclusively activated by designer drugs (DREADDs) can be expressed with silk/AAV as well to promote or suppress firing.

Silk/AAV also has potential applications for chronic extracellular recordings. The simplest application would be to use it to label cells near electrode recording sites, providing information about the morphology and projection targets of cells near the electrode tips. It could also be possible to introduce viruses for retrograde labeling to identify cells that project to the recording site. Another potentially useful variation of this is coating the tip of an optrode (optical fiber coupled to an electrode) with silk and an AAV expressing a neural activator like ChR2. If expression of the activator is made to be cell-type specific, this might prove to be a simple method to optically identify cells during extracellular electrophysiological recordings.

The potential to pattern silk/AAV in order to simultaneously express different proteins in a spatially distinct manner opens up many new types of experiments. We demonstrate that multiple viruses can be coated onto tapered fibers for depth-dependent expression of viral payloads, and it should be straightforward to extend this to different color calcium indicators, different optogenetic activity regulators, or even for anatomical purposes. The crystal skull approach, where the entire skull is replaced with a cranial window (Kim et al., 2016), might be a useful application here. Different parts of the crystal skull corresponding to different parts of the cerebral cortex can be coated with different viruses, allowing simultaneous imaging and specific manipulation of different cortical regions, all within the same animal.

EXPERIMENTAL PROCEDURES

Animals

All experimental manipulations were performed in accordance with protocols approved by the Harvard Standing Committee on Animal Care following guidelines described in the US

NIH *Guide for the Care and Use of Laboratory Animals*. C57BL/6 mice (Charles River) were used for all experiments.

Silk Fibroin Purification

Aqueous fibroin solution was prepared as described previously (Rockwood et al., 2011). Briefly, dehydrated non-living silk cocoons from *Bombyx mori* were cleaned to remove traces of worms and cut into ~1-cm^2 pieces. Pieces were boiled in 0.02 M Na2CO3 for 30 min and then rinsed with ultrapure water 3 times to remove sericin and Na_2CO_3. The resulting fibroin bundles were dried overnight and then dissolved in 9.3 M LiBr at 60°C for 4 hr (20% w/v fibroin). This solution was dialyzed against ultrapure water for 48 hr to produce aqueous fibroin solution (Slide-A-Lyzer 3–12 mL cassettes, MWCO 3500) and centrifuged twice for 20 min at 18,000 rpm. Filling dialysis cassettes fully with 12 mL resulted in the highest final concentrations of aqueous fibroin (~7.5% w/v).

Fibroin concentration was determined by measuring the final dry weight of silk films produced by casting 1 mL solution onto polystyrene weigh boats. The resulting films were ~200 μm thick, similar to the thickness of the silk/AAV films used for implant surgeries. For most experiments described in this study, fibroin was purified from cocoons generously provided by the Kaplan laboratory at Tufts University (Medford, MA) or obtained from Mulberry Farms (Fallbrook, CA). Some experiments were also performed using cocoons obtained from multiple vendors on Amazon.com, and the results were similar.

Aqueous fibroin could be stored at 4°C for up to 3 months before spontaneously forming gels. To avoid gelation, fibroin stocks were handled gently and solution was withdrawn from working aliquots. Aqueous fibroin may be stored for longer periods at −80°C, but we did not use freeze-thawed fibroin for our studies.

We have subsequently found that silk fibroin is now available commercially (5154 Sigma-Aldrich). Pilot experiments using this fibroin with tapered fibers showed expression that was qualitatively similar to that obtained using fibroin purified in our lab. Further studies are needed to determine quantitatively that extent to which the expression depends upon the source of fibroin.

Implant Surgeries

Optical fibers (Sparta et al., 2011), microendoscope lenses (Resendez et al., 2016), and cranial windows (Goldey et al., 2014) were implanted as described previously (also, see sections below). Briefly, adult mice (P40–P80) were anaesthetized with ketamine/xylazine (100/10 mg/kg) supplemented with isoflurane (1%–4%). For fibers and GRIN lenses, a craniotomy was made to accommodate the implant, and a stereotaxic device (Kopf) was used to lower implants into place slowly over 1–3 min to minimize tissue damage. For cranial windows, a craniotomy was made to accommodate the coverslip, and the implant was gently placed on top of the cortex. Implants were secured to the skull with metabond, and the wound was sutured. Buprenorphine (0.05 mg/kg) was administered after surgery subcutaneously every 12 hr for 48 hr.

Standard Fibers

Optical fiber implants were assembled using standard protocols (Sparta et al., 2011). Briefly, multimode optical fiber (Thorlabs, numerical aperature [NA] 0.39, core diameter 200 μm) was inserted into ceramic ferrules (Thorlabs, 1.25 mm outer diameter [O.D.]) and secured with epoxy. Fibers were cleaved to the desired length, and the connector end was polished.

Silk solutions were 1:1 mixtures of aqueous silk fibroin and AAV unless otherwise noted in the text. In order to minimize the volume of silk/AAV that we applied to optical components, we used stock titer virus whenever possible (titers are listed for individual viruses). Silk/AAV mixtures were loaded into a Nanoject III (Drummond), and ejected using pulled borosilicate pipettes cleaved to a small diameter (100–200 μm). The most successful configuration was to suspend the optical fiber above an inverted ejection pipette. Multiple deposits of 10 nL were applied and allowed to dry for ~60 s. To restrict expression around the fiber tip, significant care was taken to limit any contact of the silk mixture with the sides of the optical fiber. After drying at room temperature (RT) for at least 1 hr, silk/AAV-loaded implants were vacuum desiccated overnight in a vacuum chamber (25 in Hg, 4°C) and implanted the next day. To visualize silk film coatings for illustration purposes, AAV was replaced with fluorescent molecules (Texas red-dextran) and imaged under either a Zeiss AxioImager or Olympus MVX10 Macroview Scope.

To determine the extent of expression around implants, fibers were coated with silk/AAV mixtures containing AAV9.CB7.CI.eGFP.WPRE.RBG (6.4×10^{12} gc/mL, Penn Vector Core) and targeted to the striatum (anterior-posterior [AP]: 1 mm; medial-lateral [ML]: 1.75 mm). To stimulate the anterior hypothalamus, 5.2 mm optical fibers were coated with 100 nL of silk and AAV9.hSyn.ChR2(H134R).eYFP.WPRE (2.0×10^{13} gc/mL, Penn Vector Core). Fibers were implanted unilaterally into the left AHN, −1.46 mm posterior and 0.6 mm lateral to bregma. Behavioral experiments were conducted 2–3 weeks after implantation. Mice were placed into a 40 × 60 cm arena and attached via a fiber-optic commutator (Thorlabs) to a 473-nm, 50-mW DPSS analog-modulated laser (Optoengine). Light activation was 1-ms pulses at 20 Hz for 60 s. Assays were filmed with a USB camera (ELP) and scored manually.

Tapered Fibers

Lambda-B tapered optical fibers were purchased from Optogenix (Lecce, Italy). As above, 1:1 mixtures of silk and Alexa 488-dextran and/or Texas red-dextran were used to image the distribution of silk across the tapered fiber. Tapered fibers were positioned horizontally and the Nanoject positioned above the implant. ~150 nL mixture was applied by slowly “wicking” the mixture along the length of the taper in 5- to 10-nL droplets. Fibers were then vacuum desiccated overnight at 4°C. To test the ability of the coated fiber to deliver viruses, we substituted the dextrans with AAV1.CB7.CI.TurboRFP.WPRE.rBG (1.0×10^{13} gc/mL) and/or AAV1.CB7.CI.eGFP.WPRE.rBG (1.0×10^{12} gc/mL, University of Pennsylvania Vector Core) and coated them onto a Lambda-B fiber (NA 0.39, core diameter 200 μm, taper length 2.5 mm, and shank length 2 mm) for implantation into the striatum (AP: 1 mm; ML: 1.75 mm). Motor cortex (AP: 1 mm; ML: 0.5 mm) implants (NA 0.39, core diameter 200 μm, taper length 1.5 mm, and shank length 0 mm) were coated similarly, except using a

mixture of silk and AAV9.hSyn.ChR2(H134R).eYFP.WPRE (1.0×10^{13} gc/mL, University of Pennsylvania Vector Core). Histological and behavioral studies were performed at least 3 weeks after implantation.

Mice with silk-coated implants in the motor cortex were placed into a 40 × 60 cm arena for quantification of velocity and rotations induced by stimulation of opsins expressed by the silk coating. Mice were connected to a fiber optic commutator (Thorlabs) attached to a 50-mW laser (Laserglow Technologies). A 5-s, 20-Hz train of 5-ms pulses at ~3 mW was delivered every 20 ± 5 s (randomized trial intervals). Behaviors were measured in the dark using an infrared USB camera (ELP). Videos were exported into MATLAB (MathWorks), and mice positions were tracked using custom scripts and quantified.

Head-Mounted Microendoscope

1 μL of 1:1 silk and AAV8.GCaMP6s (1.0×10^{12} gc/mL, Penn Vector Core) was applied to the surface of 1.0-mm-diameter microendoscope GRIN lenses (Inscopix) by a single ejection from above. After drying overnight, lenses were implanted into dorsal striatum of 6- to 10-week-old mice (AP: 0.6 mm; ML: 2.0 mm; DV: 2.3 mm), and a baseplate for later camera attachment was fixed to the skull. 3 weeks after implantation, the GRIN lens was reversibly coupled to a miniature 1-photon microscope with an integrated 475-nm light emitting diode (LED) (Inscopix). Images were acquired at 30 Hz (nVistaHD) with the LED transmitting 0.1 to 0.2 mW of light while the mouse moved freely in an open field arena. The data were spatially down sampled by a factor of 4, and individual neuron activities were extracted using the constrained nonnegative matrix factorization for microendoscopic data (CNMFE) algorithm (Zhou et al., 2016). Extracted data were manually examined, and non-neuronal objects were removed.

Cranial Windows

Cranial windows were assembled and implanted as described previously (Goldey et al., 2014; Holtmaat et al., 2009). Briefly, a glass plug was assembled by gluing a 5-mm coverslip on top of two 3-mm coverslips (#1 thickness; CS-5R and CS-3R, Warner Instruments) using a UV-curable adhesive (Norland Optics). Unless otherwise noted, a 4-μL virus to 1 μL silk mixture was used for all cranial window studies. For initial studies, AAV9.CB7.CI.eGFP.WPRE.RBG was used to examine the breadth of expression. AAV1.Syn.GCaMP6f.WPRE.SV40 (1.0×10^{13} gc/mL, Penn Vector Core) was used for functional studies and determination of expression depth. In virus-only conditions, silk was omitted, giving a total volume of 4 μL. These solutions were carefully pipetted onto the surface of the 3-mm window and then dried at room temperature for at least 3 hr (or until the droplet was completely dried) before being implanted directly onto the brain. In contrast to the optical fiber implants discussed above, we found that vacuum desiccating coated cranial windows overnight yielded poor expression. Durectomies were performed unless otherwise stated. Care was taken during the no-durectomy conditions to preserve the integrity of the dura. Coverslips and custom-made headplates were fixed onto the brain using metabond (Parkell).

2-photon *in vivo* data were collected using a custom-built two-photon microscope with a resonant and galvanometric mirror for fast and slow scan axes respectively. Data used for single-cell fluorescence traces were acquired using a Nikon 16× 0.8 NA objective lens; data used for viewing expression across the entire window were acquired using an Olympus 4× 0.28 NA objective. Excitation was provided by a Ti:sapphire laser (Coherent) at 920 nm, delivering 50–100 mW at the sample. For comparisons between animals (Figure 5), identical power was used. Emission fluorescence was isolated using a 580-nm long-pass dichroic mirror followed by a 525/50-nm bandpass filter (Semrock) and collected by a GaAsP photomultiplier tube (Hamamatsu). Microscope control and data acquisition was managed by ScanImage 2015 (Vidrio Technologies). Images were acquired at 30 Hz with a resolution of 512 × 512 pixels.

Animals were perfused after imaging, and their brains were subsequently sliced. Tissue from cranial window animals was analyzed in ImageJ to determine fluorescence intensity across the cortex. Three coronal sections (sequential, 100-μm sections) of the anterior-most aspect of the window were quantified. For each section, three line scans (200 μm in width and at least 1.2 mm in length) were drawn from the surface of the brain to the corpus callosum in order to quantify the fluorescence in each region. All quantification was performed blind to condition, and all images were acquired under the same conditions.

Tissue Processing and Histology

Mice were anesthetized with ketamine/xylazine and transcardially perfused with PBS (pH 7.4) and 4% paraformaldehyde (PFA). Brains were post-fixed overnight at 4°C in the 4% PFA fixative solution. Tissue was sectioned coronally at 50–100 μm (Leica VT1000 S) and mounted with ProLong Diamond Anti-fade with DAPI. Slices were imaged under a 5× objective on the Zeiss Axio Imager Z2 at a fixed exposure time using MosaiX for image tiling and stitching (10% overlay). To measure the extent of expression around implants, the fiber tract was used to determine the slice nearest the tip. Expression area was determined by thresholding the fluorescence channel in ImageJ.

Supplementary Material

Refer to Web version on PubMed Central for supplementary material.

Acknowledgments

We thank D. Kaplan and C. Preda for reagents and helpful discussions and M. Ocana and the Neurobiology Imaging Center for microscopy help. We also thank J. Vazquez for illustrations and all members of the W.G.R. lab for comments on the manuscript. This facility is supported in part by the Neural Imaging Center as part of a National Institute of Neurological Disorders and Stroke (NINDS) P30 Core Center grant (NS072030). This work was supported by the GVR Khodadad Family foundation, the Nancy Lurie Marks foundation, and NIH grants NINDS R01NS032405, NINDS R21NS093498, and NINDS R35NS097284 to W.G.R.; NIMH R01MH107620 and NINDS R01NS089521 to C.D.H.; and NIMH R01 MH100568 and NINDS UU01 NS094190 to B.L.S. This work was also supported by a Canadian Institute of Health Research fellowship to S.Q.N., a National Science Foundation (NSF) Graduate Research Fellowship to S.N.C., and an NIH postdoctoral fellowship F32NS101889 to C.H.C. C.D.H. is a New York Stem Cell Foundation Robertson Neuroscience Investigator.

References

Deverman BE, Pravdo PL, Simpson BP, Kumar SR, Chan KY, Banerjee A, Wu WL, Yang B, Huber N, Pasca SP, Gradinaru V. Cre-dependent selection yields AAV variants for widespread gene transfer to the adult brain. Nat Biotechnol. 2016; 34:204–209. [PubMed: 26829320]

Fenno L, Yizhar O, Deisseroth K. The development and application of optogenetics. Annu Rev Neurosci. 2011; 34:389–412. [PubMed: 21692661]

Fernández-García L, Marí-Buyé N, Barios JA, Madurga R, Elices M, Pérez-Rigueiro J, Ramos M, Guinea GV, González-Nieto D. Safety and tolerability of silk fibroin hydrogels implanted into the mouse brain. Acta Biomater. 2016; 45:262–275. [PubMed: 27592819]

Flusberg BA, Nimmerjahn A, Cocker ED, Mukamel EA, Barretto RP, Ko TH, Burns LD, Jung JC, Schnitzer MJ. High-speed, miniaturized fluorescence microscopy in freely moving mice. Nat Methods. 2008; 5:935–938. [PubMed: 18836457]

Goldey GJ, Roumis DK, Glickfeld LL, Kerlin AM, Reid RC, Bonin V, Schafer DP, Andermann ML. Removable cranial windows for long-term imaging in awake mice. Nat Protoc. 2014; 9:2515–2538. [PubMed: 25275789]

Gradinaru V, Thompson KR, Zhang F, Mogri M, Kay K, Schneider MB, Deisseroth K. Targeting and readout strategies for fast optical neural control in vitro and in vivo. J Neurosci. 2007; 27:14231–14238. [PubMed: 18160630]

Holtmaat A, Bonhoeffer T, Chow DK, Chuckowree J, De Paola V, Hofer SB, Hübener M, Keck T, Knott G, Lee WC, et al. Long-term, high-resolution imaging in the mouse neocortex through a chronic cranial window. Nat Protoc. 2009; 4:1128–1144. [PubMed: 19617885]

Jang JH, Schaffer DV, Shea LD. Engineering biomaterial systems to enhance viral vector gene delivery. Mol Ther. 2011; 19:1407–1415. [PubMed: 21629221]

Jeong JW, McCall JG, Shin G, Zhang Y, Al-Hasani R, Kim M, Li S, Sim JY, Jang KI, Shi Y, et al. Wireless optofluidic systems for programmable in vivo pharmacology and optogenetics. Cell. 2015; 162:662–674. [PubMed: 26189679]

Kim DH, Viventi J, Amsden JJ, Xiao J, Vigeland L, Kim YS, Blanco JA, Panilaitis B, Frechette ES, Contreras D, et al. Dissolvable films of silk fibroin for ultrathin conformal bio-integrated electronics. Nat Mater. 2010; 9:511–517. [PubMed: 20400953]

Kim TH, Zhang Y, Lecoq J, Jung JC, Li J, Zeng H, Niell CM, Schnitzer MJ. Long-term optical access to an estimated one million neurons in the live mouse cortex. Cell Rep. 2016; 17:3385–3394. [PubMed: 28009304]

Knöpfel T. Genetically encoded optical indicators for the analysis of neuronal circuits. Nat Rev Neurosci. 2012; 13:687–700. [PubMed: 22931891]

Lammers JH, Kruk MR, Meelis W, van der Poel AM. Hypothalamic substrates for brain stimulation-induced patterns of locomotion and escape jumps in the rat. Brain Res. 1988; 449:294–310. [PubMed: 3395850]

Lo L, Anderson DJ. A Cre-dependent, anterograde transsynaptic viral tracer for mapping output pathways of genetically marked neurons. Neuron. 2011; 72:938–950. [PubMed: 22196330]

Madisen L, Garner AR, Shimaoka D, Chuong AS, Klapoetke NC, Li L, van der Bourg A, Niino Y, Egolf L, Monetti C, et al. Transgenic mice for intersectional targeting of neural sensors and effectors with high specificity and performance. Neuron. 2015; 85:942–958. [PubMed: 25741722]

Montgomery KL, Yeh AJ, Ho JS, Tsao V, Mohan Iyer S, Grosenick L, Ferenczi EA, Tanabe Y, Deisseroth K, Delp SL, Poon AS. Wirelessly powered, fully internal optogenetics for brain, spinal and peripheral circuits in mice. Nat Methods. 2015; 12:969–974. [PubMed: 26280330]

Mostany R, Portera-Cailliau C. A craniotomy surgery procedure for chronic brain imaging. J Vis Exp. 2008; (12):680. [PubMed: 19066562]

Packer AM, Roska B, Häusser M. Targeting neurons and photons for optogenetics. Nat Neurosci. 2013; 16:805–815. [PubMed: 23799473]

Park S, Guo Y, Jia X, Choe HK, Grena B, Kang J, Park J, Lu C, Canales A, Chen R, et al. One-step optogenetics with multifunctional flexible polymer fibers. Nat Neurosci. 2017; 20:612–619. [PubMed: 28218915]

Pisanello F, Mandelbaum G, Pisanello M, Oldenburg IA, Sileo L, Markowitz JE, Peterson RE, Della Patria A, Haynes TM, Emara MS, et al. Dynamic illumination of spatially restricted or large brain volumes via a single tapered optical fiber. Nat Neurosci. 2017; 20:1180–1188. [PubMed: 28628101]

Pritchard EM, Dennis PB, Omenetto F, Naik RR, Kaplan DL. Review physical and chemical aspects of stabilization of compounds in silk. Biopolymers. 2012; 97:479–498. [PubMed: 22270942]

Reardon TR, Murray AJ, Turi GF, Wirblich C, Croce KR, Schnell MJ, Jessell TM, Losonczy A. Rabies virus CVS-N2c(ΔG) strain enhances retrograde synaptic transfer and neuronal viability. Neuron. 2016; 89:711–724. [PubMed: 26804990]

Resendez SL, Jennings JH, Ung RL, Namboodiri VM, Zhou ZC, Otis JM, Nomura H, McHenry JA, Kosyk O, Stuber GD. Visualization of cortical, subcortical and deep brain neural circuit dynamics during naturalistic mammalian behavior with head-mounted microscopes and chronically implanted lenses. Nat Protoc. 2016; 11:566–597. [PubMed: 26914316]

Rockwood DN, Preda RC, Yücel T, Wang X, Lovett ML, Kaplan DL. Materials fabrication from Bombyx mori silk fibroin. Nat Protoc. 2011; 6:1612–1631. [PubMed: 21959241]

Runyan CA, Piasini E, Panzeri S, Harvey CD. Distinct time-scales of population coding across cortex. Nature. 2017; 548:92–96. [PubMed: 28723889]

Schek RM, Hollister SJ, Krebsbach PH. Delivery and protection of adenoviruses using biocompatible hydrogels for localized gene therapy. Mol Ther. 2004; 9:130–138. [PubMed: 14741786]

Smith GB, Fitzpatrick D. Viral injection and cranial window implantation for in vivo two-photon imaging. Methods Mol Biol. 2016; 1474:171–185. [PubMed: 27515080]

Sparta DR, Stamatakis AM, Phillips JL, Hovelsø N, van Zessen R, Stuber GD. Construction of implantable optical fibers for long-term optogenetic manipulation of neural circuits. Nat Protoc. 2011; 7:12–23. [PubMed: 22157972]

Stinson JA, Raja WK, Lee S, Kim HB, Diwan I, Tutunjian S, Panilaitis B, Omenetto FG, Tzipori S, Kaplan DL. Silk fibroin microneedles for transdermal vaccine delivery. ACS Biomater Sci Eng. 2017; 3:360–369.

Tang X, Ding F, Yang Y, Hu N, Wu H, Gu X. Evaluation on in vitro biocompatibility of silk fibroin-based biomaterials with primarily cultured hippocampal neurons. J Biomed Mater Res A. 2009; 91:166–174. [PubMed: 18780373]

Tao H, Brenckle MA, Yang M, Zhang J, Liu M, Siebert SM, Averitt RD, Mannoor MS, McAlpine MC, Rogers JA, et al. Silk-based conformal, adhesive, edible food sensors. Adv Mater. 2012; 24:1067–1072. [PubMed: 22266768]

Vepari C, Kaplan DL. Silk as a biomaterial. Prog Polym Sci. 2007; 32:991–1007. [PubMed: 19543442]

Wang L, Chen IZ, Lin D. Collateral pathways from the ventro-medial hypothalamus mediate defensive behaviors. Neuron. 2015; 85:1344–1358. [PubMed: 25754823]

Wilz A, Pritchard EM, Li T, Lan JQ, Kaplan DL, Boison D. Silk polymer-based adenosine release: therapeutic potential for epilepsy. Bio-materials. 2008; 29:3609–3616.

Zeng H, Madisen L. Mouse transgenic approaches in optogenetics. Prog Brain Res. 2012; 196:193–213. [PubMed: 22341327]

Zeng YF, Tseng SJ, Kempson IM, Peng SF, Wu WT, Liu JR. Controlled delivery of recombinant adeno-associated virus serotype 2 using pH-sensitive poly(ethylene glycol)-poly-L-histidine hydrogels. Biomaterials. 2012; 33:9239–9245. [PubMed: 23026709]

Zhang Y, Fan W, Nothdurft L, Wu C, Zhou Y, Crawford R, Xiao Y. In vitro and in vivo evaluation of adenovirus combined silk fibroin scaffolds for bone morphogenetic protein-7 gene delivery. Tissue Eng Part C Methods. 2011; 17:789–797. [PubMed: 21506685]

Zhang J, Pritchard E, Hu X, Valentin T, Panilaitis B, Omenetto FG, Kaplan DL. Stabilization of vaccines and antibiotics in silk and eliminating the cold chain. Proc Natl Acad Sci USA. 2012; 109:11981–11986. [PubMed: 22778443]

Zhou, P., Resendez, SL., Stuber, GD., Kass, RE., Paninski, L. Efficient and accurate extraction of in vivo calcium signals from microendoscopic video data. 2016. arXiv, arXiv:160507266, http://arxiv.org/abs/1605.07266

Highlights

- Silk/AAV films deposited on implants lead to localized, aligned expression
- Silk/AAV facilitates targeting small nuclei for optogenetic experiments
- Silk/AAV coatings allow continuous expression along tapered optical fibers
- Widespread expression can be achieved by coating cranial windows with silk/AAV

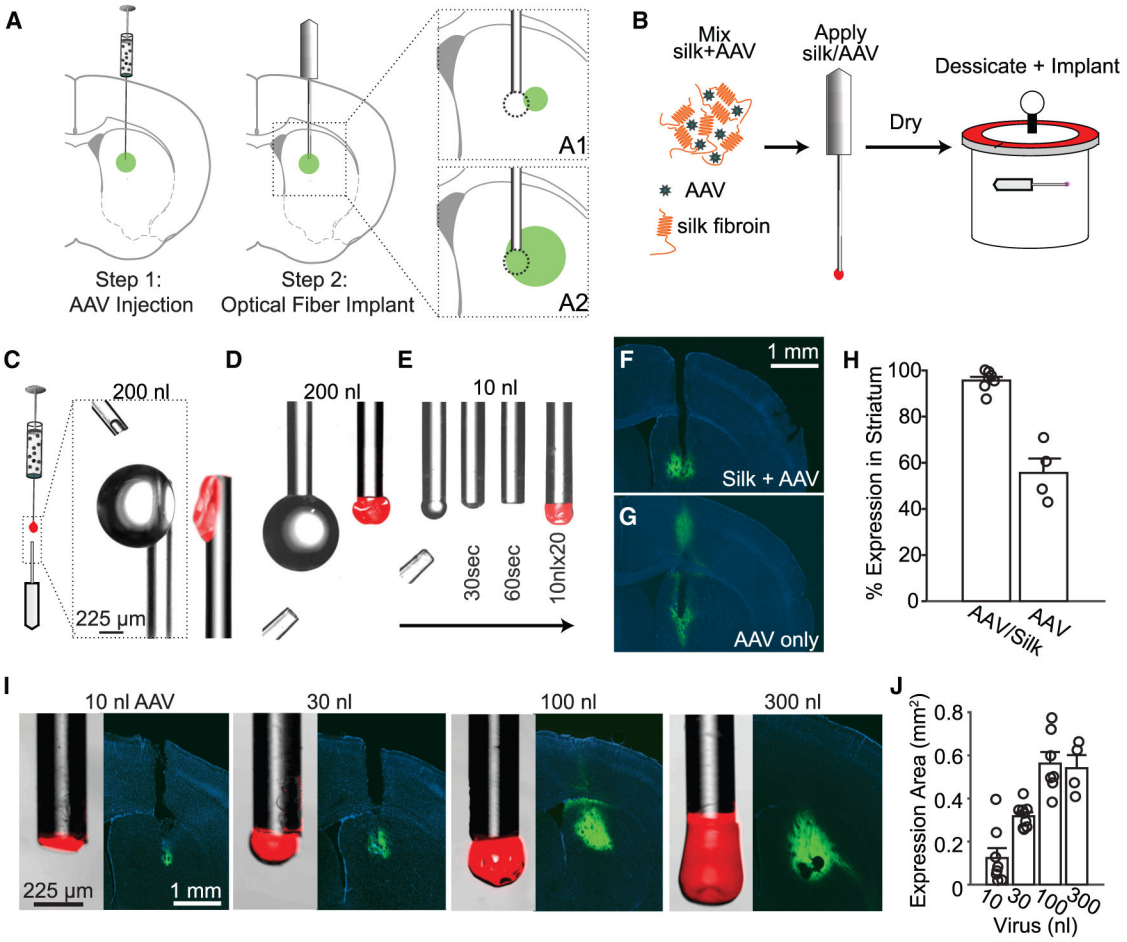

Figure 1. Silk Fibroin Is a Vehicle that Allows AAV Delivery that Is Restricted to the Tip of Optical Fibers

(A) *In vivo* optogenetic applications typically require two surgeries: first, a viral vector is injected into the target region to drive opsin expression, and second, an optical fiber is implanted to deliver light. (A1) Light will fail to drive activity in the target region if the viral injection and the implant are not aligned. (A2) If excess virus is delivered, then light may drive activity outside the target region.

(B) A suspension of silk fibroin and viral vector (silk/AAV) was applied to fiber implants and dried to produce films that release AAV after implantation.

(C) Large droplets deposited onto fibers from above often dried along the outside cladding.

(D) Large droplets deposited from below did not coat the outside of the fiber but dried into large and irregular shapes that were prone to break off during implantation.

(E) Sequential deposition of small volumes led to compact and mechanically stable dried films. (C–E) For visualization, silk was mixed with a red fluorescent dye.

(F) Representative GFP expression in the striatum 14 days after implantation of a fiber coated with silk/AAV as in (E).

(G) Example result from a fiber coated with AAV without silk.

(H) Comparison of expression following implantation of fibers coated with silk/AAV or AAV alone.

(I) Fibers showing silk/AAV labeled with red dye (left) and GFP expression patterns in the striatum following fiber implantation (right) are shown for indicated quantities of silk/AAV.
(J) Area of expression versus virus coated on implant.
Data are presented as mean ± SEM. See also Figure S1.

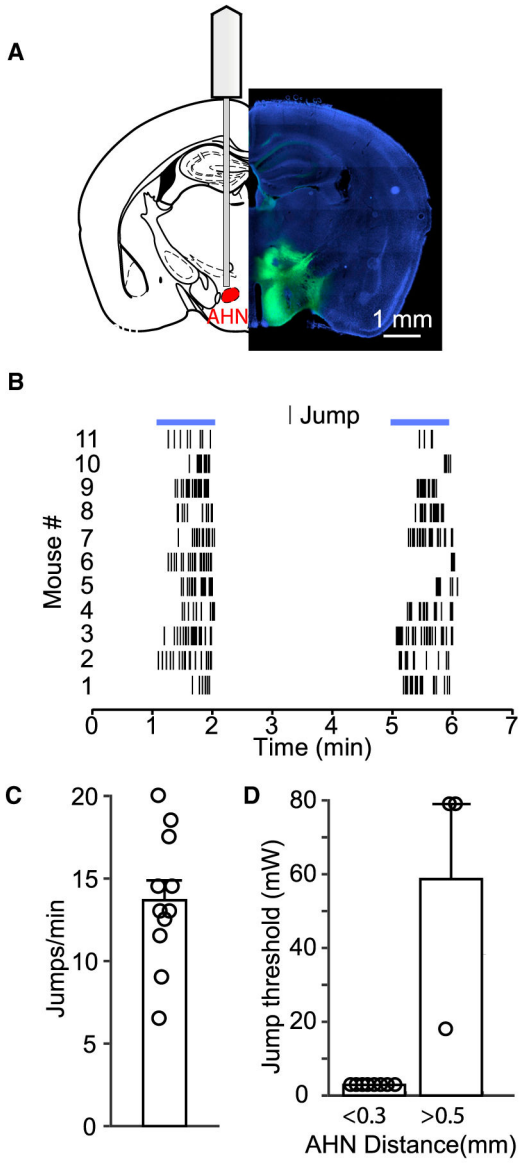

Figure 2. Silk/AAV-Coated Optical Fibers Reliably Drive Expression near the Fiber Tip and Produce Reliable Light-Evoked Behavior

(A) Fibers coated with AAV-ChR2-YFP and silk were targeted to the anterior hypothalamic nucleus (AHN) with a coronal slice showing representative ChR2-YRP expression in a mouse 4 weeks after implantation.

(B) Raster plot of jumps elicited by light activation (blue, 20 Hz, 1 ms for 60 s) in 11 mice.

(C) Average jumps per minute elicited by optogenetic stimulation.

(D) Optogenetic stimulation elicited jumping in all mice, but much lower intensities were needed to elicit jumping for implants accurately targeted to the AHN.

All data are presented as mean ± SEM. See also Movie S1.

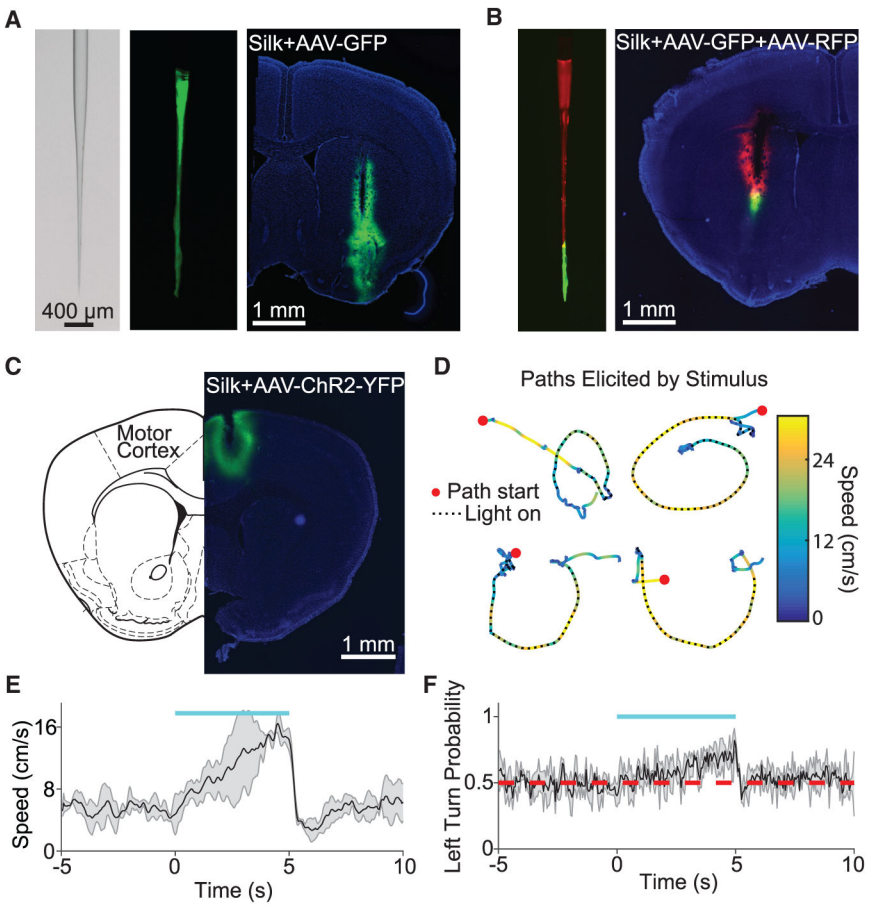

Figure 3. Tapered Optical Fibers Coated with Silk/AAV Can Drive Expression along Fibers and Can Be Used to Produce Reliable Light-Evoked Behaviors

(A) Bright-field (left) and fluorescent image (middle) of a tapered fiber uniformly coated with silk. Green fluorescent dye was added to visualize the coating. Right: fluorescent image of coronal brain slice with GFP expression in the striatum 2 weeks after implantation of an AAV-GFP coated fiber.

(B) Left: a fiber coated with silk/AAV containing green dye on the fiber tip and red dye up the shaft. Right: example implant site with a fiber used to express both RFP and GFP.

(C) Left: anatomy of a brain slice and (right) ChR2-YFP expression in the motor cortex following implantation of a tapered fiber.

(D) Stimulation of the motor cortex using a silk/AAV-ChR2-coated fiber resulted in robust turning behavior, as shown for four successive stimulations in the same mouse.

(E) Optical stimulation (blue, 20 Hz 5 ms) with silk/AAV-coated tapered fibers in the right motor cortex reliably increased the speed of locomotion in mice.

(F) Optical stimulation turned mice to the left.

All data are presented as mean ± SD. See also Movie S2.

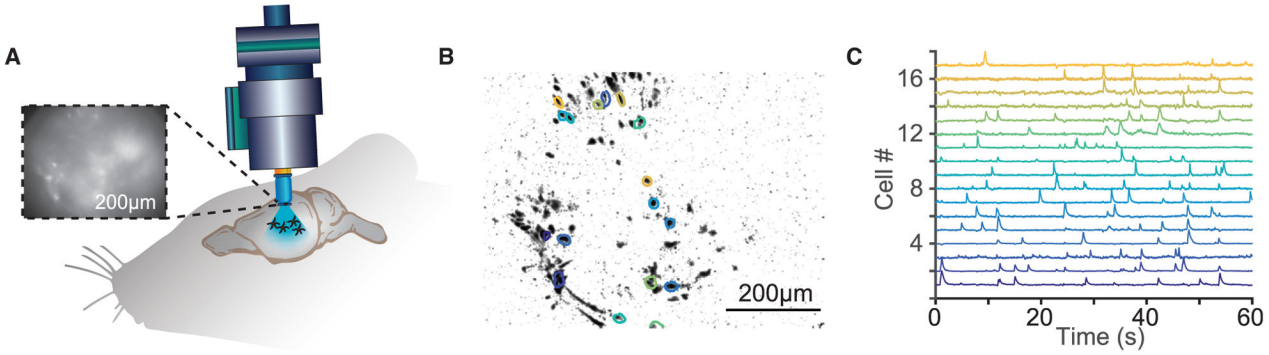

Figure 4. Expression of Calcium Indicators for *In Vivo* Mini-endoscope Imaging Is Facilitated by Coating Imaging Optical Fibers with AAV-Silk

(A) Implant schematic. 1 mm diameter endoscope lenses were coated with an AAV-GCaMP6 + silk mixture and implanted into the striatum. Raw image from an imaging session is shown in the inset.

(B) Processed image from inset in (A) showing cells and ROIs (areas circled with different colors).

(C) Example calcium transients from ROIs indicated in (B).

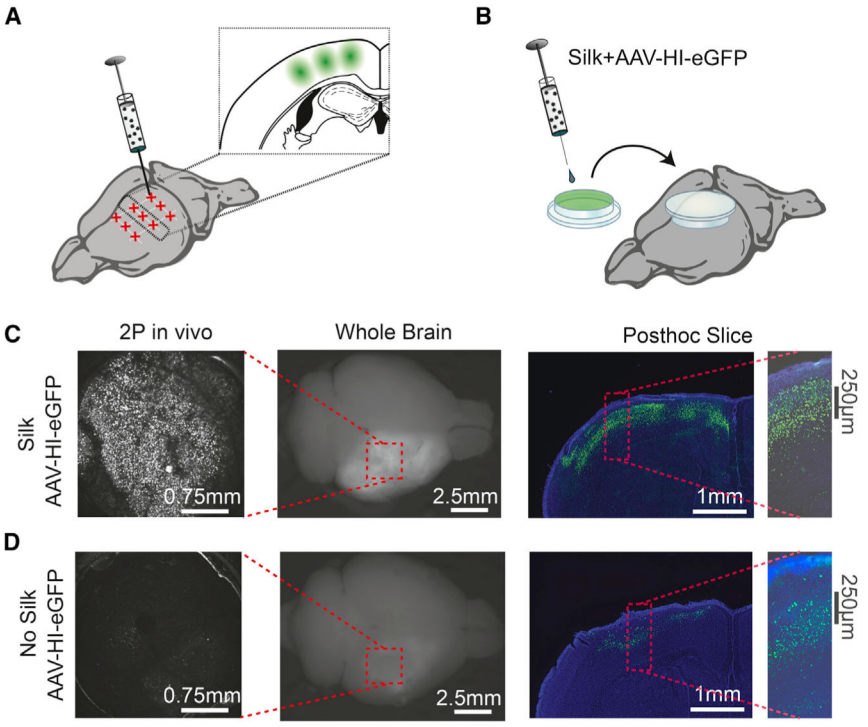

Figure 5. Widespread Cortical Expression of Fluorescent Proteins Can Be Achieved by Coating Cranial Windows with Silk and AAV

(A) The typical approach for *in vivo* two-photon imaging requires multiple virus injections. These time-consuming injections often result in non-uniform expression patterns.

(B) A mixture of silk and an AAV was dried on the surface of the cranial window to release viral vector onto the brain after implantation.

(C) Fluorescent images of GFP expression driven by a window that was coated with AAV-HI-EGFP/silk. AAV-HI-EGFP results in fluorescent labeling of somata. Left: whole brain image. Middle: in-vivo two-photon image. Right: GFP fluores-cence of a coronal section following brain removal and sectioning.

(D) As in (C), except with a coating that contained AAV-HI-EGFP only.

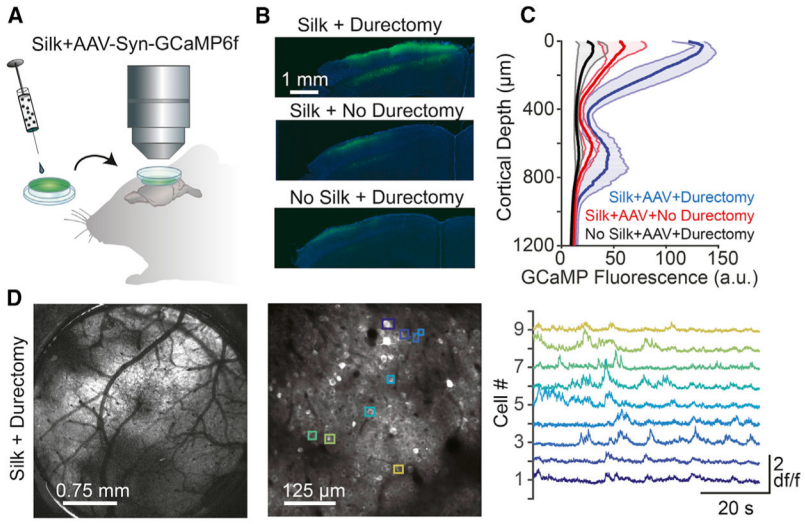

Figure 6. Silk/AAV-Coated Cranial Windows Allow Widespread Imaging of Neuronal Activity Using GCaMP6f

(A) Silk+AAV-Syn-GCaMP6f was coated on an imaging window and implanted over the cortex.

(B) GCaMP6f fluorescence is shown for acute slices cut following removal of brains.

(C) Silk/AAV-coated cranial windows resulted in expression of GCaMP6f across multiple layers of cortex. Expression was highest in durectomized animals with imaging windows coated with silk and AAV. Data are presented as mean ± SD.

(D) Left: fluorescence image through an imaging window for silk/AAV-coated windows implanted over a full durectomy. Middle: 2-photon image taken 85 μm below the cortical surface. Right: GCaMP fluorescence imaged in the ROIs highlighted in the same color. See also Figure S2 and Movie S3.